Journal of Manufacturing Systems 60 (2021) 226–238

Contents lists available at ScienceDirect

Journal of Manufacturing Systems

journal homepage: www.elsevier.com/locate/jmansys

Technical Paper

Optimal layout and reconfiguration of a fixturing system constructed from passive Stewart platforms

Timotej Gašpar [a,*], Igor Kovač [a], Aleš Ude [a,b]

[a] Humanoid and Cognitive Robotics Lab, Dept. of Automatics, Biocybernetics and Robotics, Jožef Stefan Institute, Ljubljana, Slovenia
[b] Faculty of Electrical Engineering, University of Ljubljana, Slovenia

ARTICLE INFO

Keywords:
Passive reconfigurable fixtures
Robot-supported reconfiguration
Fixture layout optimization

ABSTRACT

The distinguishing property of Reconfigurable Manufacturing Systems (RMS) is that they can rapidly and efficiently adapt to new production requirements, both in terms of their capacity and functionalities. For this type of systems to achieve the desired efficiency, it should be possible to easily and quickly setup and reconfigure all of their components. This includes fixturing jigs that are used to hold workpieces firmly in place to enable a robot to carry out the desired production processes.

In this paper, we formulate a constrained nonlinear optimization problem that must be solved to determine an optimal layout of reconfigurable fixtures for a given set of workpieces. The optimization problem takes into account the kinematic limitations of the fixtures, which are built in shape of Sterwart platforms, and the characteristics of the workpieces that need to be fastened into the fixturing system. Experimental results are presented that demonstrate that the automatically computed fixturing system layouts satisfy different constraints typically imposed in production environments.

1. Introduction

Despite the significant increase of installed robots in automated production lines in recent years, manual labor is often still necessary. In most cases, this is due to the fact that humans are more versatile, dexterous and quicker to adapt to changes in product specifications than industrial machinery. Coping with these changes in a way that does not require fluctuations in personnel is crucial in order to increase the level of automation and consequently efficiency. The Reconfigurable Manufacturing Systems (RMS) paradigm addresses these challenges and advocates for more versatile and reactive manufacturing systems [1–6].

In many production lines, there are steps in the process where workpieces must be firmly fixed to enable reliable operation of the production process and guarantee high manufacturing tolerances. Precise and rigid mounting, however, requires suitable fixturing jigs. Traditionally, fixtures are specifically designed and constructed for each workpiece. Fixture design and production is estimated to constitute 10–20% of the total production system costs [7].

Recently, we have introduced an RMS designed as a reconfigurable robot workcell aimed at automating low-batch and high-diversity production processes [8,9]. One of the key components of this system is passive reconfigurable hardware, which enables quick reconfiguration of production processes at lower costs than active systems. The newly introduced passive components do not have their own sensing or actuation systems. Instead, they can be reconfigured by a robot. Self-reconfiguration has been highlighted as the next necessary step in RMS towards the Industry 4.0 paradigm [10,11]. One of the components we developed are passive flexible fixtures called hexapods. These fixtures are built as Stewart platforms and can be reconfigured by a robot arm without long interruptions of the production process (see Fig. 3). This type of mechanism was chosen because not only it provides 6 degrees of freedom to position its top plate but also has very good load bearing properties compared to serial mechanisms [12,13].

To establish a fixturing system for a given workpiece, the hexapods' bases need to be mounted at carefully selected locations. The hexapods' top plates can then be moved by a robot to appropriate poses so that the workpiece can be firmly placed onto the established fixturing system. In the following we speak about the fixturing system *layout* when the task is to determine the locations where the hexapods' base plates are attached to the cell frame and workpieces are placed onto the fixturing system. On the other hand, we speak about hexapod *reconfiguration* when the hexapod's passive degrees of freedom are exploited to move the hexapod

* Corresponding author.
E-mail addresses: timotej.gaspar@ijs.si (T. Gašpar), igor.kovac@ijs.si (I. Kovač), ales.ude@ijs.si (A. Ude).

https://doi.org/10.1016/j.jmsy.2021.05.020
Received 8 June 2020; Received in revised form 31 May 2021; Accepted 31 May 2021
Available online 16 June 2021
0278-6125/© 2021 The Authors. Published by Elsevier Ltd on behalf of The Society of Manufacturing Engineers. This is an open access article under the CC BY license (http://creativecommons.org/licenses/by/4.0/).

top plate to a new desired pose. While the reconfiguration of hexapods can be performed without human intervention, their mounting within the cell cannot. It is therefore important that the mounting locations of fixtures are determined in such a way that it is possible to reconfigure the hexapods into postures that allow the placement of all given workpieces. In general, the determination of hexapod layout is tedious, time consuming, and often difficult or even impossible to achieve manually. The task becomes increasingly challenging as the number of hexapods and workpieces gets larger. Fig. 1 shows an example where two workpieces can be held by the fixturing system without re-mounting the bases of the three hexapods holding both workpieces. Only the top plates of the hexapods need to be moved when replacing one workpiece with another.

In this paper, we present the design of passive Stewart platforms suitable for constructing a fixturing system with passive degrees of freedom and formulate a constrained nonlinear optimization problem that must be solved to determine the optimal layout of the fixturing system (constructed from hexapods) for a given set of workpieces. The main highlights of the developed fixturing system and the optimization approach are:

- By solving the proposed constrained nonlinear optimization problem, we obtain the mounting poses of the hexapods so that all workpieces can be placed onto the fixturing system without repositioning the bases of the hexapods.
- By introducing various constraints into the optimization process, the system can avoid kinematic limits of hexapods, collisions between fixtures and workpieces, and workcell boundaries.
- For any given workpiece, the computed postures of the hexapods can be established by a robot, which moves the hexapods' top plates without any human intervention.

The paper is structured as follows: we start with the related work in Section 2, followed by the introduction of the developed flexible fixtures and their kinematic model in Section 3. Next in Sections 4 and 5 we formulate a nonlinear optimization problem to compute the layout of the flexible fixtures and the constraints that need to be fulfilled by the fixtures and workpieces. The results of the evaluation are presented in Section 6, while the discussion and concluding remarks are provided in Sections 7 and 8.

2. Related work

The application of dedicated fixtures in industrial processes with a high workpiece variability is expensive because many fixtures need to be designed to account for all possible variations. A better alternative is to apply reconfigurable fixtures, which can be classified in two groups: modular and flexible fixtures [14]. Modular fixtures are usually composed of different smaller modules that can be arranged in an appropriate configuration to enable the placement of a given workpiece. Flexible fixtures, which are in focus of this study, are usually ready-to-use mechanisms with one or more degrees of freedom. They can be reconfigured in order to ensure solid placement of different workpieces in the cell [15].

Some flexible fixturing systems allow for automatic reconfiguration, either by internal actuators or external manipulation [16,17]. Automatic reconfiguration of fixtures increases the precision of their positioning, removes the need for human intervention, and lowers change-over times. Using the Stewart platform design, two similar concepts of passive flexible fixtures have been proposed in the past by Gödl et al. [18] and Jonnson et al. [19]. The former design, dubbed hexapod in this paper, was used in practical manufacturing setups described in [9]. In most cases, more than one hexapod is needed to fix the desired workpiece, which makes the determination of optimal location and posture of hexapods an important but difficult to compute problem.

An important issue that is often considered when optimizing fixture layouts is how to accurately place a workpiece onto a fixture. Some researchers focused on sheet metal workpieces [20–22], yet others on more rigid workpieces [23–25]. All of these methods determine a set of locating (anchor) points where a fixturing system establishes contacts with a given workpiece. Other researchers went a step further and investigated the determination of locating points on the workpiece for production processes with multiple workstations [26] or involving multiple workpieces [27]. Tadic et al. developed a special device to measure the tangential forces acting on a workpiece and the resulting displacement in order to study different clamping/locating elements for machining operations [28]. All these works address a different problem than our research, where the main topic of investigation is how to place and configure a fixturing system so that multiple workpieces can be mounted onto it. However, the above methods can be used to determine the locating points on each workpiece, which must be provided to fully specify the proposed optimization problem.

Kong and Ceglarek [29] point out another important issue in reconfigurable assembly, which is how to determine the layout of locating points for a family of parts so that the functional work envelope of a fixturing system is minimized. Unlike in our approach, they do not consider the actual kinematics of the fixturing system and therefore cannot compute the placement and postures of the fixturing elements.

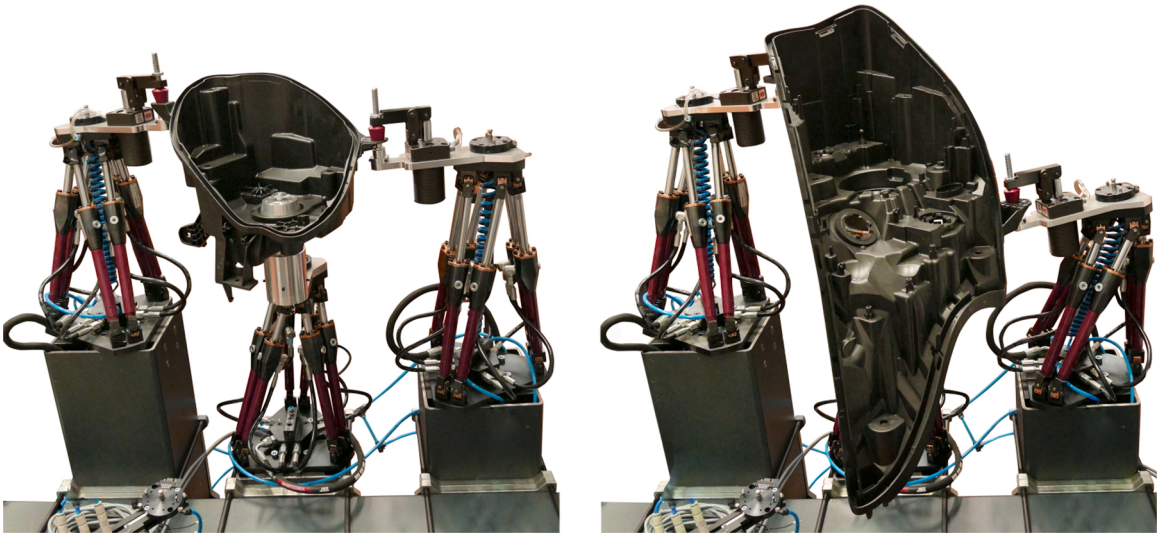

Fig. 1. The fixturing system made of passive Stewart platform (hexapods) holding two different automotive light housings without the need to re-position their bases.

Other authors used actuated Stewart platforms as reconfigurable fixtures [30,31]. However, instead of focusing on the placements and postures of the Stewart platforms, they focused on optimizing the mechanism's design to achieve the desired characteristics.

The determination of the placement of various devices within a robotic cell has also received a considerable research attention in the past [32–40]. Most authors studied the optimal placement of the robots within a predefined cell, in some cases also taking into account the peripheral equipment. Yet others were interested where to place a workpiece so that the robot has the highest stiffness during machining operations on the said workpiece [32]. Some authors even took into account a human worker participating in the co-production process and considered the ergonomic aspects of the human worker while performing the tasks alongside the robot [41]. Naturally, the developed optimization criteria vary significantly depending on the desired outcome (cycle time, layout area, reachability, energy consumption, etc.).

It is evident from the above review that the main distinguishing property of our approach is the ability to optimize both the placement and posture of a fixturing system for *multiple* workpieces. Neither research that focuses on single workpieces nor the works that deal with the placement of different peripheral elements to optimize the workcell layout can adequately address this problem. Moreover, none of the papers that specifically investigated the fixturing systems made of Stewart platforms tackle the issue of their placement in the cell and multiple workpieces. It was therefore deemed necessary to develop a new solution for our problem – the determination of locations of the base and top plates of a set of Stewart platforms so that it is possible to firmly mount a given set of workpieces onto the fixturing system while taking into account different workspace constraints so that the robot is able to execute the desired operations. To the best of our knowledge, the proposed solution is the first of its kind.

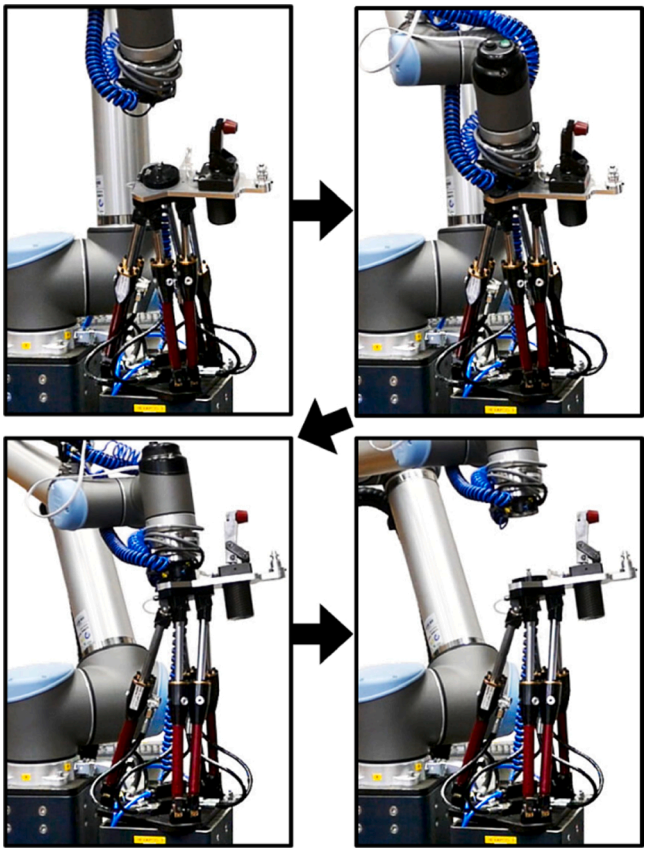

Fig. 3. Reconfiguration sequence.

3. Passive reconfigurable fixtures

The design of passive reconfigurable fixtures used in this paper, here called hexapods, stems from the design proposed by [18]. The developed hexapods are composed of two plates, top and bottom, connected by 6 extendable legs. The base plate is typically affixed to the cell's frame, while the top plate is where the fixturing elements (centering pins, clamps, etc.) are installed. Thus, the top plate comes in contact with the workpiece. Additionally, the tool end of the tool-exchange system is mounted on the top plate so that the robot can latch onto it when performing reconfiguration (see Figs. 2 and 3). There are no actuators or displacement sensors in the extendable legs, which makes our hexapods relatively inexpensive to produce. Each leg has a hydro-mechanical brake that ensures that the hexapod is stiff when engaged and compliant when disengaged. Up to this point, the design does not diverge much from the one proposed by [19]. The distinguishing feature of our hexapod design are the special Cardan joints with an adjustable backlash mechanism [42], which ensure high stiffness when the breaks are engaged. This type of hexapods were used to construct a fixturing system also in our previous work [8,9], but at that time the locations and postures of hexapods had to be determined manually for each workpiece.

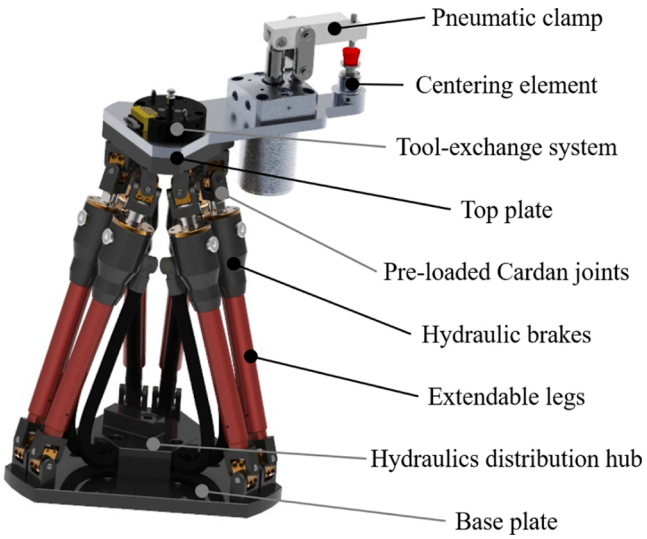

Fig. 2. The hexapod design.

3.1. Kinematic model of the Stewart platform

The hexapod's workspace is limited. To ensure that different workpieces can be placed onto a fixturing system consisting of several hexapods, the mounting location of each hexapod needs to be carefully selected. We can use the hexapod's inverse kinematics to determine if any given pose of the top plate is within its workspace. Even though the kinematic model of a 6-UPU parallel mechanism is well known [43], we briefly describe it in this section to facilitate the development of the optimization algorithm.

Let's denote the pose of the hexapod base described in the world coordinate system o by $\mathrm{B} \in \mathbb{R}^{4\times4}$ and the pose of the hexapod top plate relative to the base plate coordinate system b by $\mathrm{T} \in \mathbb{R}^{4\times4}$ (see Fig. 4). We further denote the mounting point of the k/th leg on the hexapod base by $\mathrm{v}_{b,k} \in \mathbb{R}^3$ (in the hexapod base coordinate frame b) and the mounting points of the leg on the top plate by $\mathrm{v}_{t,k} \in \mathbb{R}^3$ (in the top plate coordinate frame t). The vector from $\mathrm{v}_{b,k}$ to $\mathrm{v}_{t,k}$ can be computed as

$$\begin{bmatrix} \mathrm{l}_{b,k} \\ 0 \end{bmatrix} = -\begin{bmatrix} \mathrm{v}_{b,k} \\ 1 \end{bmatrix} + \mathrm{T}\begin{bmatrix} \mathrm{v}_{t,k} \\ 1 \end{bmatrix} \tag{1}$$

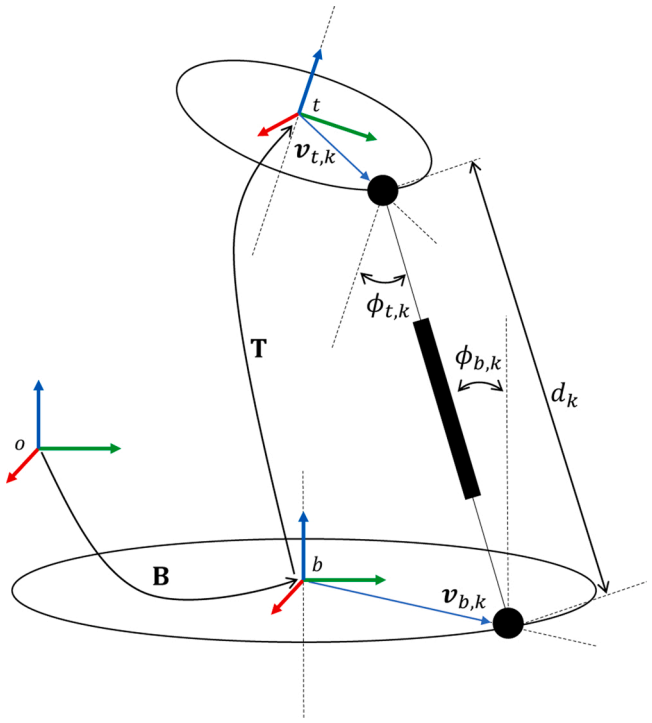

Fig. 4. Kinematic model of the flexible fixture – Stewart platform.

$l_{b,k} \in \mathbb{R}^3$ is the position of the k/th leg in the hexapod base coordinate system. We can convert this vector from Cartesian to spherical coordinates (see A.1 for the equations):

$$l_{b,k} \xrightarrow{\text{Cartesian to spherical}} [d_k, \rho_k, \psi_k] \tag{2}$$

Conveniently, the coordinate d_k represents the length of the k/th leg. In actuated parallel mechanisms, this is usually the driven internal coordinate. However, to compute whether a given top plate pose is within the reachable workspace of the hexapod, we also need to calculate the angle between the leg and the z axis of both the hexapod base and top plate coordinate system.

The angle between the k/th leg and the z axis of the hexapod base can be calculated as follows:

$$\phi_{b,k} = \frac{\pi}{2} - \rho_k \tag{3}$$

To calculate the angle $\phi_{t,k}$ between the z-axis of the top plate coordinate system t and the k/th leg, we can use the dot product between the normalized vector of the k/th leg and the third column of rotation matrix R, where

$$T = \begin{bmatrix} R & t \\ 0 & 1 \end{bmatrix} \tag{4}$$

We obtain:

$$\phi_{t,k} = arccos\left(\frac{1}{d_k} l_{b,k}^T R_3\right) \tag{5}$$

This way we can compute the internal coordinates for all legs of the parallel mechanism $\{d_k, \phi_{b,k}, \phi_{t,k}\}_{k=1}^6$ as a function of the top plate pose T

$$[d_k \quad \phi_{t,k} \quad \phi_{b,k}]^T = f_k^{IK}(T), \quad k = 1, \ldots, 6, \tag{6}$$

where each f_k^{IK} takes into account the end-positions $v_{b,k}$ and $v_{t,k}$ of the k/th leg in the local coordinate systems. To ensure that the pose of the top plate is in the hexapods's workspace, each of these coordinates must be within a specified range

$$d_{k,\min} \le d_k \le d_{k,\max}, \quad \phi_{t,k,\min} \le \phi_{t,k} \le \phi_{t,k,\max}, \quad \phi_{b,k,\min} \le \phi_{b,k} \le \phi_{b,k,\max}. \tag{7}$$

These limits should be taken into account when computing the optimal placement of hexapods and workpieces.

3.2. Transformation between poses of hexapods and workpieces

To compute the placements and configurations of hexapods so that all workpieces can be mounted onto the resulting fixturing system, we need to relate the hexapod and workpiece poses. This arrangement is illustrated in Fig. 5. We denote the homogeneous transformation matrices – expressed in the world coordinate system – of the j/th workpiece and the i/th hexapod as $W_j \in \mathbb{R}^{4\times4}$ and $B_i \in \mathbb{R}^{4\times4}$, respectively. Let M be the number of workpieces that need to be placed onto the fixturing system and N the number of hexapods forming the fixturing system. Each workpiece should be attached to the top plate of each hexapod in the fixturing system at a predefined anchor point. We denote the transformation between the j/th workpiece coordinate frame and the anchor point to be attached to the i/th hexapod as $A_{i,j}$, $i = 1,\ldots,N$, $j = 1,\ldots,M$. The indices of the hexapods and anchor points coincide because the number of hexapods is the same as the number of anchor points on the workpiece. Furthermore, we denote the transformation from the i/th hexapod's base to its top plate by $T_{i,j}$ and the pose of the centering element on the top plate, where the workpieces are mounted on the hexapod, by C_i.

To close the kinematic chain in Fig. 5, we also introduce a rotational degree of freedom at the anchor points. This way we can account for conical centering elements and circular anchor points, where orientation is not fully constrained. We obtain

$$D_{i,j}(\vartheta_{i,j}) = \begin{bmatrix} R(\vartheta_{i,j}) & 0 \\ 0 & 1 \end{bmatrix}, \quad R(\vartheta_{i,j}) = \begin{bmatrix} cos(\vartheta_{i,j}) & -sin(\vartheta_{i,j}) & 0 \\ sin(\vartheta_{i,j}) & cos(\vartheta_{i,j}) & 0 \\ 0 & 0 & 1 \end{bmatrix} \tag{8}$$

These degrees of freedom only exist for conical centering elements. For non-conical centering elements we can set $D_{i,j} = I$, $\vartheta_{i,j} = 0$.

We can now relate the poses of the i/th hexapod base and top plate to the pose of the j/th workpiece. We obtain the following relationship (see Fig. 5)

$$T_{i,j} = B_i^{-1} W_j A_{i,j} D_{i,j}(\vartheta_{i,j})^{-1} C_i^{-1}. \tag{9}$$

Here $A_{i,j}$ and C_i are constant transformations usually obtained from the CAD models of hexapods and workpieces.

4. Optimization of a fixturing system layout

A fixturing system is usually constructed from two or more hexapods. Eq. (9) shows that the layout of such a fixturing system (the location and configuration of hexapods) is fully specified by determining the poses of the hexapod base plates $B_i \in \mathbb{R}^{4\times4}$, the poses of workpieces $W_j \in \mathbb{R}^{4\times4}$ to be placed onto the fixturing system, and the rotational angles $\vartheta_{i,j}$ at anchor points. The angles are necessary only in case of conical centering elements, whereas they are not needed with centering elements that fully specify the orientation of the workpiece with respect to the hexapod, e.g. rectangular centering elements. From these data, the poses of hexapod top plates $T_{i,j} \in \mathbb{R}^{4\times4}$ can be computed using Eq. (9). In this section we consider how to compute the optimal layout when the fixturing system is built from N hexapods and there are M workpieces that should be firmly placed onto the hexapods. This should be accomplished by only moving the top plates of the hexapods and without moving their base plates.

For this purpose we derive an optimization problem to compute B_i, W_j, and $\vartheta_{i,j}$. We start by expressing orientations with a minimal number of mutually independent parameters. One such representation are Euler

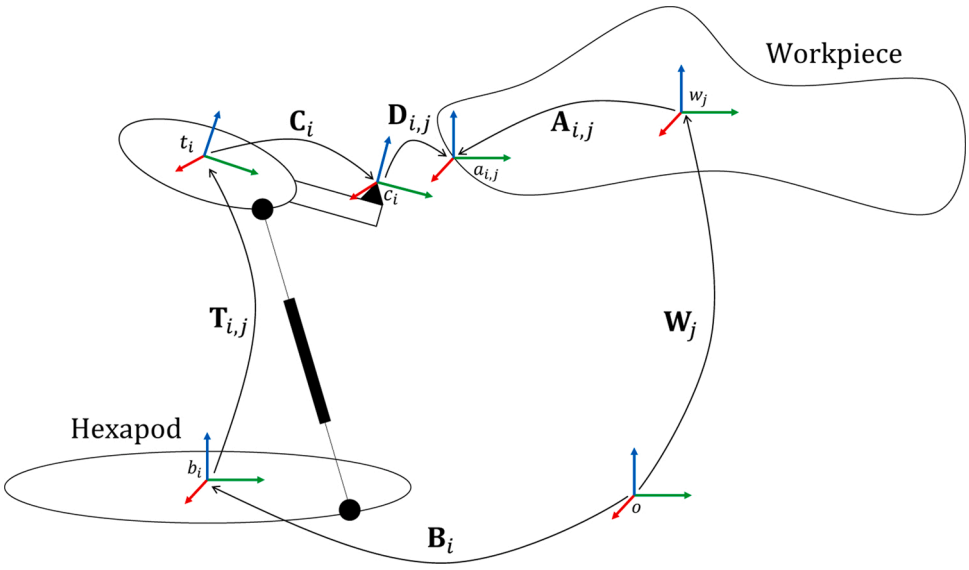

Fig. 5. The kinematic chain between the jth workpiece and the ith hexapod.

angles, which represent orientation as a combination of three elemental rotations around orthogonal axis. We denote the Euler angles as α,β,γ. In terms of Euler angles, the transformation matrices B_i and W_j can be represented by

$$\mathrm{p}_i^b = \begin{bmatrix} x_i^b & y_i^b & z_i^b & \alpha_i^b & \beta_i^b & \gamma_i^b \end{bmatrix}^{\mathrm{T}}, \tag{10}$$

$$\mathrm{p}_j^w = \begin{bmatrix} x_j^w & y_j^w & z_j^w & \alpha_j^w & \beta_j^w & \gamma_j^w \end{bmatrix}^{\mathrm{T}}. \tag{11}$$

Let $\boldsymbol{f}^{\mathrm{Eul}}$ be the function mapping the poses expressed in terms of Euler angles into homogeneous matrices (see A.2). Using Eq. (9), we can express the pose of the top plate $\mathrm{T}_{i,j}$ in terms of p_i^b, p_j^w, and $\vartheta_{i,j}$

$$\begin{aligned} \mathrm{T}_{i,j} = \mathrm{T}_{i,j}(\mathrm{p}_i^b, \mathrm{p}_j^w, \vartheta_{i,j}) &= \begin{bmatrix} \mathrm{R}_{i,j}(\mathrm{p}_i^b, \mathrm{p}_j^w, \vartheta_{i,j}) & \mathrm{t}_{i,j}(\mathrm{p}_i^b, \mathrm{p}_j^w, \vartheta_{i,j}) \\ 0 & 1 \end{bmatrix} \\ &= \boldsymbol{f}^{\mathrm{Eul}}(\mathrm{p}_i^b)^{-1} \boldsymbol{f}^{\mathrm{Eul}}(\mathrm{p}_j^w) \mathrm{A}_{i,j} \mathrm{D}_{i,j}(\vartheta_{i,j})^{-1} \mathrm{C}_i^{-1} \\ &= \boldsymbol{f}_{i,j}^{\mathrm{rel}}\left(\mathrm{p}_i^b, \mathrm{p}_j^w, \vartheta_{i,j}\right) \end{aligned} \tag{12}$$

To formulate an optimization problem to compute the hexapod layout, we need to specify a suitable criterion function. One possible choice is to prefer workpiece poses that are close to the neutral poses specified by the production cell designer. We denote these poses, expressed in world coordinate system, as

$$\mathrm{W}_{0,j} = \begin{bmatrix} \mathrm{R}_{0,j}^w & \mathrm{t}_{0,j}^w \\ 0 & 1 \end{bmatrix} \tag{13}$$

Another possible criterion is to prefer the hexapod configurations that are close to the neutral posture of the hexapod, which we define as

$$\mathrm{T}_0 = \begin{bmatrix} \mathrm{I} & \mathrm{t}_0^t \\ 0 & 1 \end{bmatrix}, \quad \mathrm{t}_0^t = \begin{bmatrix} 0 & 0 & z_0 \end{bmatrix}^{\mathrm{T}}. \tag{14}$$

T_0 can also be viewed as the pose of the hexapod top plate expressed in the coordinate system of the bottom plate. The constant z_0 can be determined from the kinematic model of the hexapod. When the top plate is at this pose, the load bearing properties of the hexapod are good and its legs are well separated from each other. Consequently, the possibility of collisions between the legs when the top plate is moved by a robot is reduced when starting from this pose.

Based on Eqs. (12), (13), (14) and (A.4), we defined the following criterion function

$$\begin{aligned} c(\mathrm{p}_i^b, \mathrm{p}_j^w, \vartheta_{i,j}) &= \lambda_o \left(\sum_{j=1}^{M} \| \mathrm{t}(\mathrm{p}_j^w) - \mathrm{t}_{0,j}^w \|^2 + \lambda_r \| log\left(\mathrm{R}\left(\mathrm{p}_j^w\right) \mathrm{R}_{0,j}^{w\,\mathrm{T}} \right) \|^2 \right) \\ &\quad + \sum_{j=1}^{M} \sum_{i=1}^{N} \| \mathrm{t}_{i,j}(\mathrm{p}_i^b, \mathrm{p}_j^w, \vartheta_{i,j}) - \mathrm{t}_0^t \|^2 + \lambda_r \| log\left(\mathrm{R}_{i,j}\left(\mathrm{p}_i^b, \mathrm{p}_j^w, \vartheta_{i,j}\right) \right) \|^2, \end{aligned} \tag{15}$$

where $\lambda_r,\ \lambda_o > 0$ are the scaling factors. Note that the rotation matrix logarithm is used to estimate the distance between two orientations (see A.3). λ_r governs the trade-off between position and orientation accuracy, which are given in different units (meters and radians, respectively). It was set to 0.1 in our experiments to ensure the appropriate balance between the position and orientation accuracy. λ_o balances the precision of the desired workpiece pose and the desired relative top plate pose. Since the units are the same in this case, its value can be set to 1 in the absence of task-specific information. In general, the optimal values for these two parameters must be tuned in a trial-and-error process.

The criterion function (15) ranks better the hexapod layouts where the workpieces are closer to their user-specified desired poses (first term) and where the hexapods are closer to their neutral postures (second term). Keeping the top plates as close as possible to their neutral poses makes sure that the hexapods are as far as possible from their kinematic limits. This is important in order to avoid violating these limitations during the hexapod reconfiguration, when the top plate is moved from one posture to another by a robot. However, if only this term was considered, the fixturing system could be placed anywhere in 3-D space. The first term therefore makes sure that the workpieces are placed as close as possible to the initially specified workpiece poses. Otherwise there would exist multiple solutions where the fixturing system was simply translated and rotated in 3-D space.

Not every combination of hexapod base plate locations and workpiece poses results in a valid solution for a fixturing system. Only those combinations for which the corresponding poses of the top plates computed by Eq. (9) are within the workspaces of all hexapods forming the fixturing system are valid. As explained in Section 3.1, any valid solution fulfills nonlinear constraints (7). Using Eqs. (9) and (12), we can rewrite Eq. (6) as follows

$$\begin{bmatrix} d_k \\ \phi_{t,k} \\ \phi_{b,k} \end{bmatrix} = \boldsymbol{f}_k^{\mathrm{IK}}\left(\boldsymbol{f}_{i,j}^{\mathrm{rel}}(\mathrm{p}_i^b, \mathrm{p}_j^w, \vartheta_{i,j}) \right) \tag{16}$$

Furthermore, we need to limit the orientations $\mathrm{R}_{i,j}(\mathrm{p}_i^b, \mathrm{p}_j^w, \vartheta_{i,j})$ of the

hexapods' top plates to prevent collisions between the legs of hexapods, which occur when top plates rotate too much. We denote the maximum allowed rotation of hexapod top plates by $\xi_{\max} > 0$. We can therefore formulate the following optimization problem

$$\arg\min_{\mathrm{p}_i^b, \mathrm{p}_j^w, \vartheta_{i,j}} c\left(\mathrm{p}_i^b, \mathrm{p}_j^w, \vartheta_{i,j}\right)$$

$$\text{subject to} \begin{cases} \begin{bmatrix} d_{k,\min} \\ \phi_{t,k,\min} \\ \phi_{b,k,\min} \end{bmatrix} \leq \boldsymbol{f}_k^{\mathrm{IK}}\left(\boldsymbol{f}_{i,j}^{\mathrm{rel}}(\mathrm{p}_i^b, \mathrm{p}_j^w, \vartheta_{i,j})\right) \leq \begin{bmatrix} d_{k,\max} \\ \phi_{t,k,\max} \\ \phi_{b,k,\max} \end{bmatrix} \\ \| \, log(\mathrm{R}_{i,j}(\mathrm{p}_i^b, \mathrm{p}_j^w, \vartheta_{i,j})) \, \| \leq \xi_{\max} \end{cases} \tag{17}$$

$$k = 1, \ldots, 6, \quad i = 1, \ldots, N, \quad j = 1, \ldots, M.$$

The above optimization problem has altogether $6(M+N) + \mathrm{MN}$ variables and 37MN nonlinear inequality constraints that need to be fulfilled.

5. Additional constraints to influence the fixturing system layout

In this section we provide some additional constraints that may be added to the optimization problem (17) to compute a better solution.

5.1. Preventing overlap between the base plates of the hexapods

We can define additional constraints to ensure that the base plates of the hexapods do not overlap. Let a_h be the radius of the hexapods' base plates. The base plates of two hexapods do not overlap if the following constraint is fulfilled

$$\mathrm{d}(\mathrm{p}_i^b, \mathrm{p}_l^b) = \sqrt{(x_i^b - x_l^b)^2 + (y_i^b - y_l^b)^2} \geq a_h, \tag{18}$$

where $i = 1,\ldots,N$, $l = i+1,\ldots,N$. This should hold true for every pair of hexapods. Thus, we must add $\binom{N}{2}$ constraints of the form (18) to the optimization problem (17) to prevent the bases of the hexapods from overlapping.

5.2. Limiting the area where workpieces and hexapods can be placed

By specifying the lower and upper bounds for optimization variables p_i^b, p_j^w, and $\vartheta_{i,j}$, we can limit the area in the workspace where the hexapods and workpieces may be placed. We define both the lower and upper bounds for the optimization problem (17)

$$\mathrm{p}_{i,\min}^b \leq \mathrm{p}_i^b \leq \mathrm{p}_{i,\max}^b, \tag{19}$$

$$\mathrm{p}_{j,\min}^w \leq \mathrm{p}_j^w \leq \mathrm{p}_{j,\max}^w, \tag{20}$$

$$\vartheta_{i,j,\min} \leq \vartheta_{i,j} \leq \vartheta_{i,j,\max}. \tag{21}$$

The lower and upper bounds are usually defined based on the information about the location where the desired production task needs to be performed. This depends on the placement of the robot in the workspace, but can also be influenced by other production process specifications. Note that by setting the lower and upper bounds to the same value, we can lock any degree of freedom in the optimization process. However, care must be taken when defining the values of these boundaries. They should be set so that they do not restrict the search area to such a degree, where a feasible solution to the optimization problem (17) does not exist.

In our practical applications, there was only one interval for each variable. However, if some of the variables could take values in several disjoint intervals, we could formulate multiple optimization problems for each interval combination. The best result would then be obtained by comparing these multiple solutions with respect to the value of criterion function (15).

5.3. Collision avoidance

The above constraints are insufficient to prevent collisions between workpieces and hexapods. In order to calculate collisions between workpieces and hexapods, the CAD models of both must be available. In CAD models, objects are usually composed of a set of planar polygons and the distance between two objects is computed by determining the minimum distance between polygons belonging to two different objects [44,45]. For each hexapod-workpiece pair, we denote the distance between the two as $\Gamma(\mathcal{H}_i, \mathcal{W}_j)$, where $\mathcal{H}_i$ and $\mathcal{W}_j$ denote the i/th hexapod and the j/th workpiece, respectively. Thus to ensure that there are no collisions between hexapods and workpieces, we can add the following constraints to the optimization problem (17)

$$\Gamma(\mathcal{H}_i(\mathrm{p}_i^b, \mathrm{p}_j^w, \vartheta_{i,j}), \mathcal{W}_j(\mathrm{p}_j^w)) \geq \Delta, \tag{22}$$

where $i = 1,\ldots,N$, $j = 1,\ldots,M$, and $\Delta > 0$ is the minimum allowed distance between the hexapods and workpieces. As there are MN hexapod-workpiece pairs, we obtain MN additional constraints this way.

The addition of constraints (22) significantly increases the computational time of optimization problem (17) because the calculation of the distance between two free-form objects is computationally expensive. Care must therefore be taken when deciding whether or not to add these constraints.

6. Experimental evaluation

We evaluated several aspects of the developed fixturing system and optimization algorithm: (1) influence of constraints on the final layout of the fixturing system, (2) computation time with different numbers of hexapods and workpieces, and (3) collision prevention when computing optimal layouts. The first two experiments were carried out with a simulated workpiece while the last was based on a real experimental setup from the automotive industry. In all experiments we set λ_r, λ_o and $\xi_{\max}$ to the following values: $\lambda_r = 0.1$, $\lambda_o = 1$ and $\xi_{\max} = \frac{\pi}{6}$. Additionally, in all experiments the initial values of the optimization variables were set as follows: $\mathrm{p}_j^w = [0,0,0,0,0,0]^{\mathrm{T}}$, $\vartheta_{i,j} = 0$. The desired workpiece poses were set to $\mathrm{W}_{0,j} = \mathrm{I}$. The initial guesses for p_i^b were calculated by taking the average over positions and Euler angles obtained from bottom plate poses $\mathrm{B}_{0,i,j}$, which were calculated by rearranging formula (9) for all workpieces, $j = 1,\ldots,M$,

$$\mathrm{B}_{0,i,j} = \mathrm{W}_{0,j}\mathrm{A}_{i,j}\mathrm{D}_{i,j}(0)^{-1}\mathrm{C}_i^{-1}\mathrm{T}_0^{-1}. \tag{23}$$

The optimization procedure was implemented in MATLAB using the nonlinear programming solver *fmincon*.

The simulated workpiece was designed as a modular object that can be assembled in different configurations (Fig. 6). The object consists of a main hexagonal plate to which six extension arms labeled from *a* - *f* (Fig. 6a) can be attached. The extension arms have two holes on the side that is attached to the main plate and one hole as an anchor point on the other side that is in in contact with the hexapod (Fig. 6b). They can be mounted either facing up or down. This design allowed us to mount the extension arms at different edges and thus obtain many different workpieces. An example simulated workpiece with 3 extension arms is displayed in Fig. 6c.

6.1. Choice of optimization algorithm

Different algorithms for solving constrained nonlinear optimization problem can be applied to solve (17) in practical applications. We have evaluated the performance of three state-of-the-art algorithms, which

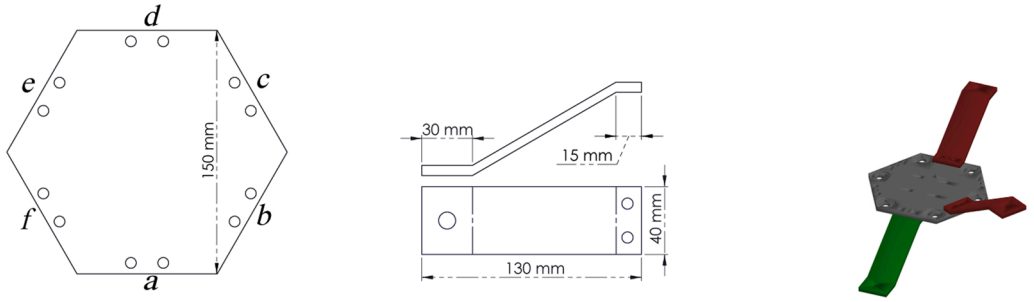

(a) Top view of the modular workpiece base with measures.

(b) Top and side view of the modular workpiece arm with dimensions.

(c) A 3-D render of a workpiece example.

Fig. 6. The simulated modular workpiece used to evaluate the developed method.

are provided as part of Matlab Optimization Toolbox under the following names: (a) Active Set algorithm [46] (b) Sequential Quadratic Programming (SQP) algorithm [47] and (c) Interior Point algorithm [48]. The evaluation was conducted on 20 experimental setups with four hexapods and three workpieces randomly constructed from the modular workpiece described above ($N = 4$ and $M = 3$). All algorithms were initialized with the same starting point. The average computation times and the average final values of the criterion function (17) together with their standard deviations are presented in Table 1.

In our experimental evaluation, all three algorithms converged to the final estimate before reaching the specified maximum number of iterations (400). The results in Table 1 show that on average, the Interior Point algorithm was more computationally efficient but found solutions with slightly higher final values of criterion function (15). On the other hand, the SQP algorithm achieved the lowest final values of (15) but took the most time. The Active Set algorithm was somewhere in between but closer to SQP. Note that the standard deviation of computation times is rather large, thus it is not always the same algorithm which is the fastest. As for the resulting layouts, all three algorithms succeeded to find configurations that satisfy all the specified constraints. However, as evident from Fig. 7, different algorithms find different local minima and therefore the resulting (all valid) layouts can be slightly different.

We decided to use the Interior Point algorithm in the rest of our experiments due to its computational efficiency.

6.2. Influence of constraints on the fixturing system layout

We first studied how the inclusion of different constraints affects the resulting layout of the fixturing system. The experiments in this section were all carried out on a set of 3 workpieces with 4 anchor points each. Thus, four hexapods were required to firmly hold each workpiece. We started by applying the optimization problem (17) without any additional constraints. The results are show in Figs. 8 and 9 where the top-down and side views of the resulting layouts are displayed. In the remainder of this section we will show how including different constraints to the optimization problem affects resulting layouts and compare these layouts to Figs. 8a and 9a, which show the top and side view of the fixturing system for the same workpiece.

Table 1
Comparing the performance of different nonlinear constrained optimization algorithms when applied to solving the optimization problem (17).

	Active set	SQP	Interior point
Average computation time	6'42"	11'34"	5'49"
Computation time standard dev.	2'17"	3'48"	2'57"
Average final values of (15)	0.678	0.666	0.733
Final values standard dev.	0.130	0.134	0.138

Often we need to make sure that the hexapods are mounted on a planar support surface. Assuming that the support surface is an $x-y$ plane with $z = 0$, we can add the following constraints to the optimization problem (17)

$$\begin{cases} z_i^b = 0 \\ \alpha_i^b = \beta_i^b = 0 \end{cases}, \quad i = 1,2,3,4. \tag{24}$$

Note that these constraints are of type (19) introduced in Section 5.2. The selected optimization algorithm can handle such box constraints for the optimization variables well [48]. The fixturing system layout computed with these additional constraints is shown in Fig. 10a, where the hexapods are displayed from a side view. This result demonstrates that the hexapods are placed as desired, i.e. located on the support plane at $z = 0$ with the base plates parallel to the planar surface. In comparison, the hexapod base plates in Fig. 9a, where the layout was computed without considering constraints (24), are neither placed at $z = 0$ nor are their base plates parallel to the support plane. Additionally, the poses of the workpieces are displaced along the z-axis compared to their poses in Fig. 9a. This is an expected result because without lifting the workpieces the algorithm could not satisfy constraints (24).

In the next experiment we introduced additional constraints with respect to the location of the base plates on the support plane

$$\begin{cases} -0.2 \le x_i^b \le 0.2 \\ -0.2 \le y_i^b \le 0.2 \end{cases}, \quad i = 1,2,3,4. \tag{25}$$

Fig. 10b shows that the hexapods are now closer together compared to Fig. 8a, but two of them overlap. To prevent overlaps, we next introduced the constraint of type (18), i.e.

$$\sqrt{(x_i^b - x_l^b)^2 + (y_i^b - y_l^b)^2} \ge 0.28, \quad i = 1,2,3,4, \quad l = i+1,\ldots,4. \tag{26}$$

The fixturing system layout computed by including constraints (26) is depicted in Fig. 10c. It keeps the hexapods' coordinate frame origins within the limits specified by constraints (25) while preventing the hexapod base plates from overlapping.

The above results demonstrate that by adding various constraints we can greatly affect the computed layouts. Sometimes just solving the original optimization problem without any constraints can result in a viable layout. However, to guarantee that the hexapods are placed within the robot's workspace at sensible orientations and without overlapping, it is often necessary to introduce additional constraints, which ensure that the computed layouts are physically viable and can be easily constructed.

6.3. Computation time and number of hexapods and workpieces

The aim of our next experiment was to evaluate how increasing the

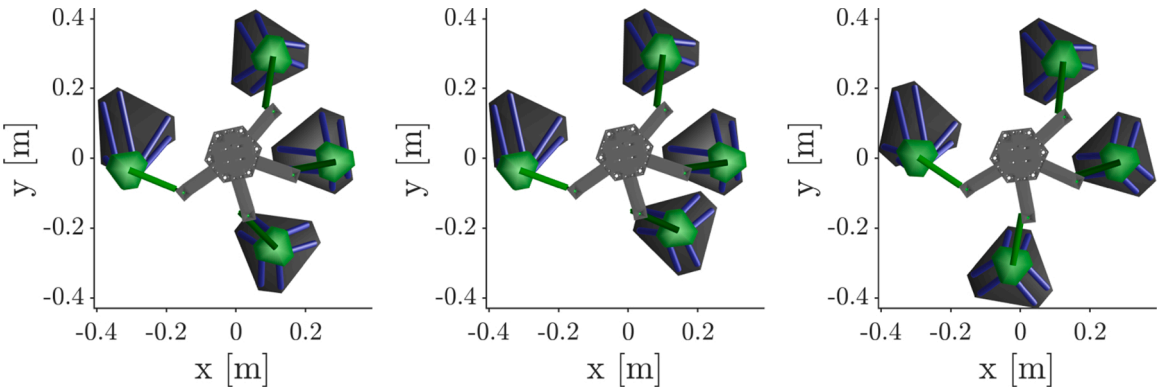

Fig. 7. Top-down view of a solution for the same workpiece and hexapods obtained by three different optimization algorithms (from left to right): Active Set, SQP, and Interior Point.

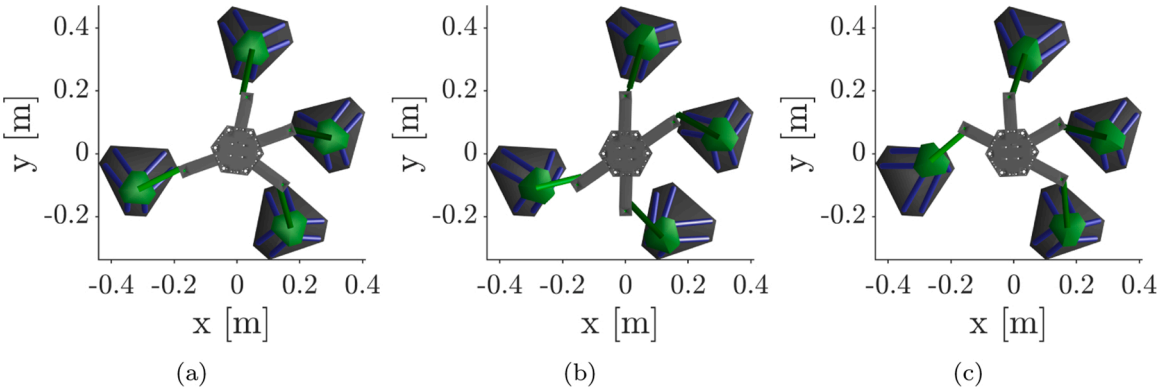

Fig. 8. Top-down views of the fixturing system layout for three different workpieces (a, b & c) computed by optimizing (17) and without considering any additional constraints.

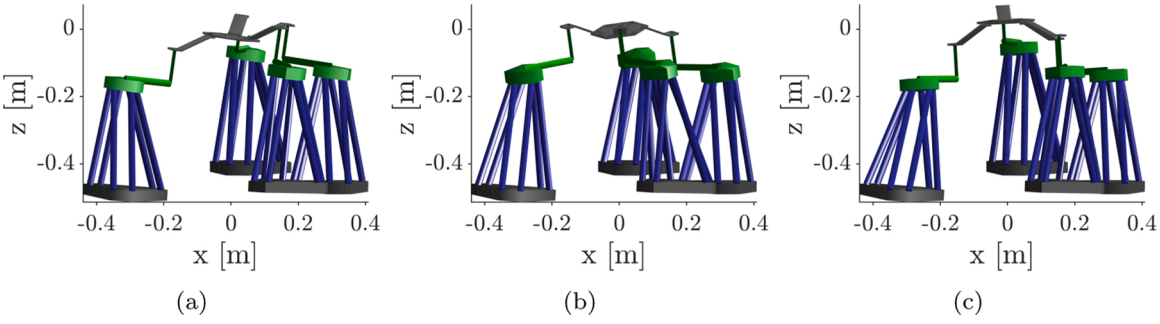

Fig. 9. Side view of the layout depicted in Fig. 8.

number of workpieces and hexapods influences the computation time needed to solve the associated optimization problem. We performed optimization for layouts with $M = 2, \ldots, 6$ workpieces and $N = 3, \ldots, 6$ hexapods (or anchor points), thus altogether 20 different layouts. The arrangement of anchor points on each modular workpiece (Fig. 6) was randomly selected. The optimization processes were halted when the relative change of the optimization variables p_i^b, p_j^w and ϑ_{ij} was smaller than 10^{-3}. For each layout, we solved optimization problem (17) with additional constraints defined in Eq. (18) to prevent overlap between the hexapods' base plates. The optimization procedure was executed on a desktop computer with the 4th generation Intel Core i7-4790K CPU having 4 cores running at 4.00 GHz base frequency and 16 GB of RAM.

The bar graph shown in Fig. 11a illustrates the computation time needed to solve each optimization problem, whereas the bar graph in Fig. 11b presents the time needed for one evaluation of the criterion function and constraints. As expected, smaller numbers of workpieces and hexapods result in lower computation times. These results show that it is possible to solve optimization problems with small number of workpieces and hexapods in a matter of minutes. On the other hand, it might take up 45 minutes to solve more complex optimization problems.

6.4. Collision prevention

In the third experiment we evaluated the developed method in an experiment originating in the automotive industry. In our previous work, we presented the assembly of different automotive headlights in a reconfigurable robot workcell without needing to manually rearrange the placement of fixtures [9]. The assembly is showcased in Fig. 12. There were two workpieces held by the fixturing system constructed from three hexapods. However, unlike in our current work, the layout of

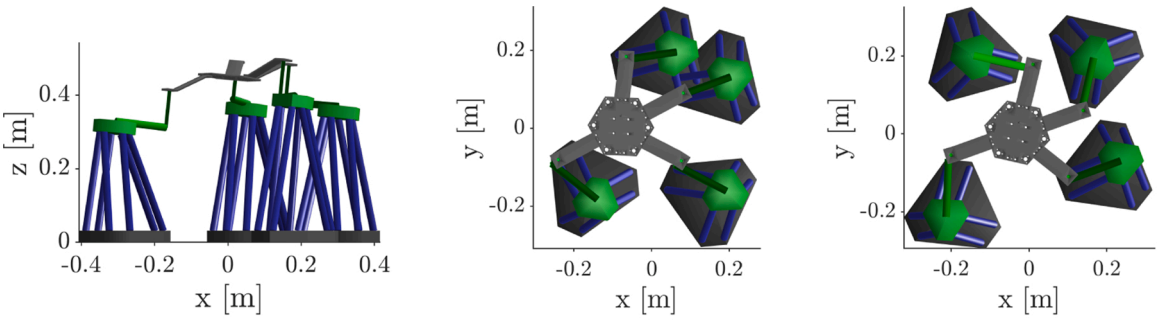

(a) Results when including constraints (24) of type (19).

(b) Results when including constraints (24) and (25), both of type (19).

(c) Results when including constraints (24), (25), (26) of type (19) and (18).

Fig. 10. The effect of gradually adding constraints defined by Eqs. (24), (25), and (26) to the optimization problem (17) for the workpiece shown in Figs. 8a and 9a.

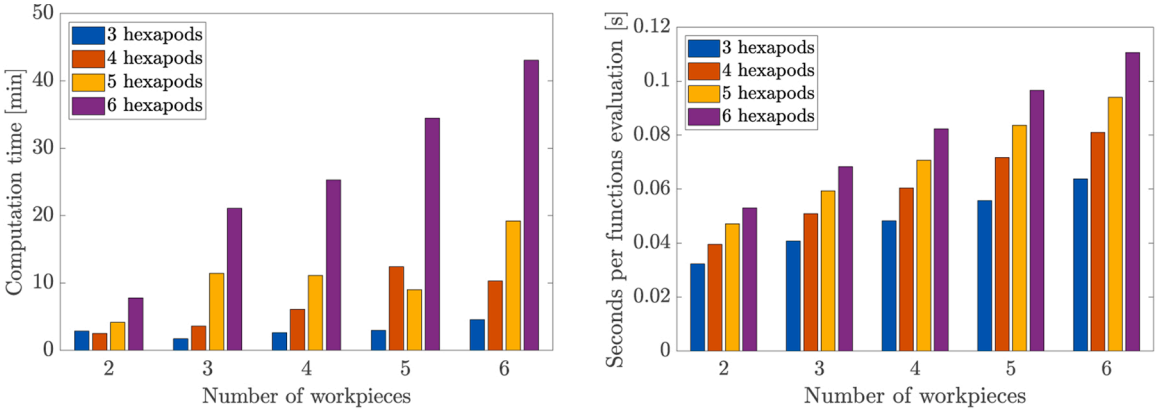

(a) Computation time of the optimization algorithm.

(b) Computation time for each evaluation of the criterion function and constraints.

Fig. 11. Influence of the number of hexapods (equal to the number of anchor points) and workpieces on the computation time.

the fixturing system had to be determined manually in [9].

While the shape of the simulated workpiece is rather simple, the shapes of the real automotive headlights are much more complex. This can cause collisions between workpieces and hexapods in otherwise valid layouts. We can address this issue by adding collision avoidance constraints (22) to optimization problem (17). In this experiment, the distance between two objects was computed using the algorithm described in [44] with Δ from constraint (22) set to $\Delta = 0.001$. To enforce that there are no collisions between the hexapods' base plates and that the hexapods are placed within the robot's workspace, we also added constraints (18) and (19), (20), respectively.

Fig. 13 shows the results of optimization in the case when collision constraints were not considered. In the computed layout, both workpieces are in collision with one of the hexapods. The system was able to compute collision-free layouts when the collision constraints were added (Fig. 14). However, in this case the computation time increased significantly. Without the collision constraints, it took 1'27" with 45 optimization iterations to solve the optimization problem, whereas with the collision constraints it took 11'52" with 37 optimization iterations. Thus, the inclusion of the collision constraints increased the

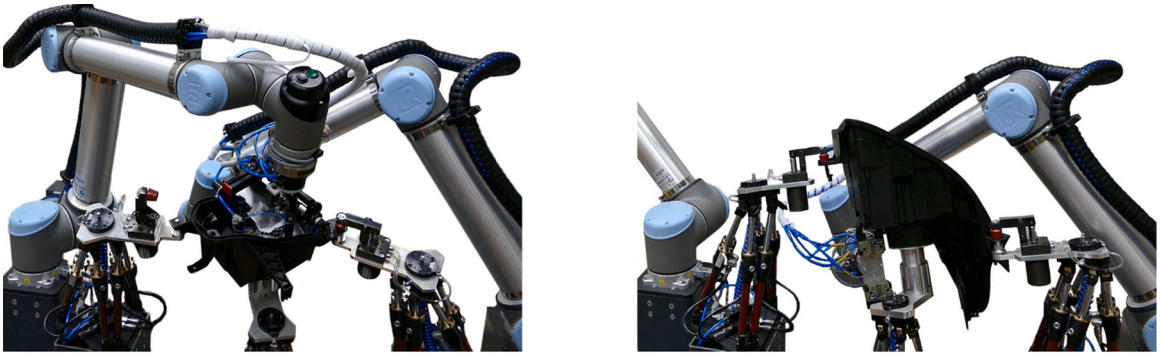

(a) Smaller headlight assembly.

(b) Bigger headlight assembly.

Fig. 12. Two robots performing assembly operations on two different automotive headlights while the headlights are firmly held by the fixturing system.

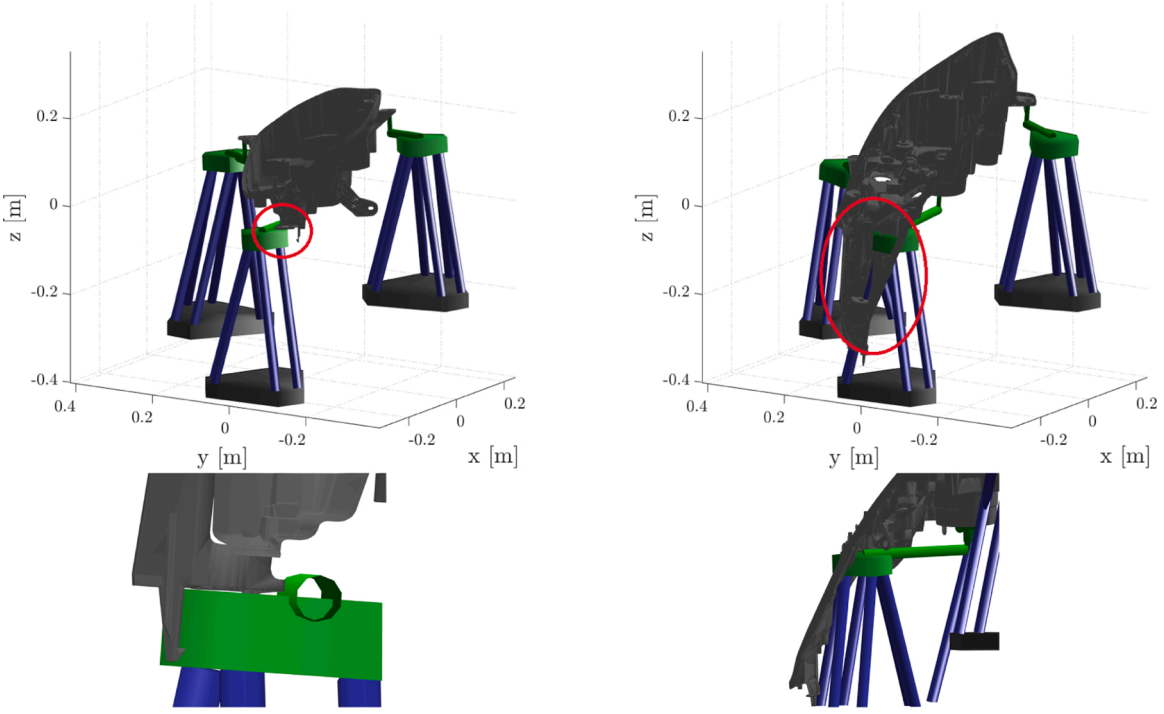

(a) Fixturing system layout for the smaller headlight with the collision point marked and zoomed-in.

(b) Fixturing system layout for the bigger headlight with the collision point marked and zoomed-in.

Fig. 13. The fixturing system layouts for two different models of automotive headlights. The two layouts can be established by automatic reconfiguration without moving the hexapods' base plates. The collision prevention constraints were not used in this case. While the result is kinematically correct, both workpieces collide with one of the hexapods.

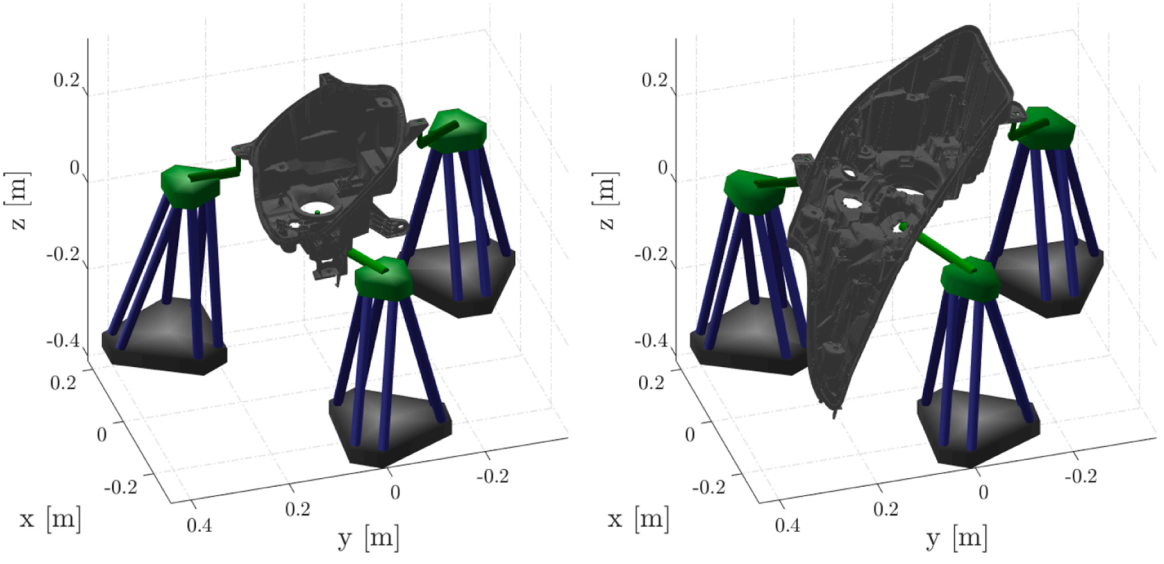

Fig. 14. Collision free layouts of the fixturing system for two different automotive headlight models. The collision prevention constraints were used to compute these layouts.

computation time by approx. 820%.

7. Discussion

One important factor to consider when it comes to the collision prevention constraint is how to choose an appropriate collision detection algorithm. The algorithm applied in our experiments does not calculate the penetration depth between two objects. This can considerably hinder the performance of the optimization algorithm because the algorithm cannot estimate the derivative of the collision constraint once the objects are in collision. It is therefore important to select the initial values for p_i^b, p_j^w and ϑ_{ij} in such a way that there are no collisions. This way the optimization algorithm can calculate the derivative of the distance between objects in every iteration and therefore work as intended.

Since the hexapods are Stewart platforms with six degrees of

freedom, their top plates can be moved to any desired position and orientation within their workspace. However, the extent of each hexapod's workspace is limited by the length of the hexapod's legs. Because of this limitation, there are sets of workpieces for which it is not possible to compute the fixturing system layout so that all workpieces could be placed onto the fixturing system without moving the hexapods' base plates to different locations. For example, if the sizes of two workpieces are very different, then the distances between anchor points will also be very different for both workpieces. In such cases it is impossible to place the base plates of the hexapods in such a way that the hexapods' top plates could reach the anchor points of both workpieces without moving the base plates. The optimization process runs until it reaches the maximum allowed number of iterations as specified by the user. Upon reaching this maximum, it alerts the user that it could not satisfy all the specified constraints.

The criterion function applied in the developed optimization method was defined to compute layouts where the workpieces are close to the poses specified by production cell designer and the hexapods' top plates are close to their neutral pose. Depending on the production task, a different criterion function could be selected. For example, in a collaborative cell we could define a criterion function that takes into account different factors related to the well being and performance of a human worker [49]. Yet another possibility is to include the properties of a robot operating in the cell into the optimization process, e.g. energy consumption [50]. One should be aware, however, that the optimization problem becomes more complex and consequently more computationally expensive as the number of variables increases. The definition of additional criterion functions and constraints is the topic for our future research.

8. Conclusion

In this paper we presented the design of an innovative fixturing system built from Stewart platforms (hexapods) with passive degrees of freedom. The hexapods have no sensors or actuators but can be autonomously reconfigured to different postures by a robot. We formulated an optimization problem that takes into account the kinematics of the Stewart platforms and the geometry of workpieces that need to be mounted into the fixturing system. The purpose of the developed optimization problem is to determine the placement and posture of passive fixtures in the reconfigurable workcell so that different workpieces can be mounted without the need to manually relocate the hexapods. The developed optimization problem can take into account several different constraints, including kinematic constraints of hexapods, overlap between the hexapod base plates, and collisions between hexapods and workpieces. The constraint to prevent overlap between the bases of hexapods might seem redundant because the collision prevention constraint could also solve this issue. However, it is much less computationally expensive to detect the overlap between the hexapod bases than to evaluate whether or not two free-form objects collide.

An important advantage of the proposed approach is that we only need inverse kinematics of the hexapods to compute the kinematic constraints of the fixturing system. This is crucial to keep the computation time low because direct kinematics of a Stewart platform is difficult to compute, with solutions involving polynomials of 40th degree [51].

We evaluated our approach in a series of experiments involving simulated workpieces and two different headlights from the automotive industry. We showed that by solving the proposed constrained nonlinear optimization problem, we can compute the fixturing system layout that is guaranteed to be within the physical limits of the workcell while avoiding collisions between the hexapods and/or workpieces. However, adding different constraints increases the computational time significantly.

Acknowledgement

This work has received funding from the program group P2-0076 Automation, robotics and biocybernetics supported by the Slovenian Research Agency and from the EU's Horizon 2020 grants TRINITY (grant agreement no. 825196) and CoLLaboratE (grant agreement no. 820767).

Declaration of Competing Interest

The authors declare that they have no known competing financial interests or personal relationships that could have appeared to influence the work reported in this paper.

Appendix A. Auxiliary mathematics

To facilitate the reproduction of results presented in this paper, we provide here the formulas used to compute inverse kinematics of the Stewart platform via spherical coordinates, Euler angles used to represent orientation, and the matrix logarithm used to compute the distance between two orientations.

A.1 Spherical coordinates

Given a 3-D point expressed in Cartesian coordinates $[x, y, z]$, the mapping to spherical coordinates $[x, y, z] \xrightarrow{\text{Cartesian to spherical}} [d, \rho, \psi]$ is defined as follows:

$$d = \sqrt{x_2 + y_2 + z^2}, \tag{A.1}$$

$$\rho = arctan\left(\frac{y}{x}\right), \tag{A.2}$$

$$\psi = arctan\left(\frac{\sqrt{x^2 + y^2}}{z}\right) \tag{A.3}$$

A.2 Euler angles

Euler angles represent orientation as a combination of three elemental rotations around the coordinate axes. There are twelve possible sequences of elemental rotations to express general orientation [52]. We chose the rotations around the $x - y - z$ sequence of rotation axes. Function f^{Eul}, which

maps the 6-D pose $\mathrm{p} = [x, y, z, \alpha, \beta, \gamma]^{\mathrm{T}}$ into a homogeneous transformation matrix, is defined as:

$$\begin{aligned} \boldsymbol{f}^{\mathrm{Eul}}(\mathrm{p}) &= \begin{bmatrix} c_\beta c_\gamma & -c_\beta s_\gamma & s_\beta & x \\ c_\alpha s_\gamma + c_\gamma s_\alpha s_\beta & c_\alpha c_\gamma - s_\alpha s_\beta s_\gamma & -c_\beta s_\alpha & y \\ s_\alpha s_\gamma - c_\alpha c_\gamma s_\beta & c_\gamma s_\alpha + c_\alpha s_\beta s_\gamma & c_\alpha c_\beta & z \\ 0 & 0 & 0 & 1 \end{bmatrix} \\ &= \begin{bmatrix} \mathrm{R}(\mathrm{p}) & \mathrm{t}(\mathrm{p}) \\ 0 & 1 \end{bmatrix}, \end{aligned} \tag{A.4}$$

where s_* and c_* denote the sines and cosines of Euler angles α, β and γ.

A.3 Logarithmic mapping of a rotation matrix

The rotation matrix logarithm is defined as follows [53]

$$log(\mathrm{R}) = \begin{cases} [0, \quad 0, \quad 0]^{\mathrm{T}}, & \mathrm{R} = \mathrm{I} \\ \theta \boldsymbol{n}, & \text{otherwise} \end{cases},$$
$$\theta = arccos\left(\frac{\mathrm{trace}(\mathrm{R}) - 1}{2}\right), \quad \boldsymbol{n} = \frac{1}{2sin(\theta)} \begin{bmatrix} r_{32} - r_{23} \\ r_{13} - r_{31} \\ r_{21} - r_{12} \end{bmatrix} \tag{A.5}$$

The components of $log(\mathrm{R}) \in \mathbb{R}^3$ are called exponential coordinates of R. This representation of orientation is commonly referred to as axis-angle representation. Note that $\| log(\mathrm{R}) \| = |\theta|$ because $\boldsymbol{n}$ is a unit vector. For $\theta = \pm\pi$ we cannot compute $\boldsymbol{n}$ using the above formula because in this case off-diagonal terms do not provide information about the rotation axis (which is nevertheless defined up to a sign ambiguity). However, we can still compute $\| log(\mathrm{R}) \| = |arccos(-1)| = \pi$, thus the norm $\| log(\mathrm{R}) \|$ is defined for all $\mathrm{R} \in \mathrm{SO}(3)$. It can be used to define a metric on SO(3), $\mathrm{d}(\mathrm{R}_1, \mathrm{R}_2) = \| log(\mathrm{R}_2 \mathrm{R}_1^{\mathrm{T}}) \|$. Note that $\mathrm{d}(\mathrm{I}, \mathrm{R}) = \| log(\mathrm{R}) \|$.

References

[1] Koren Y, Heisel U, Jovane F, Moriwaki T, Pritschow G, Ulsoy AG, et al. Reconfigurable manufacturing systems. CIRP Ann – Manuf Technol 1999;48(2):527–40.
[2] ElMaraghy HA. Flexible and reconfigurable manufacturing systems paradigms. Int J Flex Manuf Syst 2005;17(4):261–76.
[3] Bi ZM, Lang SYT, Shen W, Wang L. Reconfigurable manufacturing systems: the state of the art. Int J Prod Res 2008;46(4):967–92.
[4] Andersen A-L, Brunoe TD, Nielsen K, Rösiö C. Towards a generic design method for reconfigurable manufacturing systems. J Manuf Syst 2017;42:179–95.
[5] Zheng C, Qin X, Eynard B, Bai J, Li J, Zhang Y. SME-oriented flexible design approach for robotic manufacturing systems. J Manuf Syst 2019;53:62–74.
[6] Bortolini M, Ferrari E, Galizia FG, Regattieri A. An optimisation model for the dynamic management of cellular reconfigurable manufacturing systems under auxiliary module availability constraints. J Manuf Syst 2021;58:442–51.
[7] Bi ZM, Zhang WJ. Flexible fixture design and automation: review, issues and future directions. Int J Prod Res 2001;39(13):2867–94.
[8] Gašpar T, Ridge B, Bevec R, Bem M, Gosar Ž, Kovač I, et al. Rapid hardware and software reconfiguration in a robotic workcell. In: 18th international conference on advanced robotics (ICAR); 2017. p. 229–36.
[9] Gašpar T, Deniša M, Radanovič P, Ridge B, Savarimuthu TR, Kramberger A, et al. Smart hardware integration with advanced robot programming technologies for efficient reconfiguration of robot workcells. Robot Comput-Integr Manuf 2020;66(101979):1–17.
[10] Bortolini M, Galizia FG, Mora C. Reconfigurable manufacturing systems: literature review and research trend. J Manuf Syst 2018;49:93–106.
[11] Morgan J, Halton M, Qiao Y, Breslin JG. Industry 4.0 smart reconfigurable manufacturing machines. J Manuf Syst 2021;59:481–506.
[12] Zhang D, Lang SY. Stiffness modeling for a class of reconfigurable PKMs with three to five degrees of freedom. J Manuf Syst 2004;23(4):316–27.
[13] Bem M, Deniša M, Gašpar T, Jereb J, Bevec R, Kovač I, et al. Reconfigurable fixture evaluation for use in automotive light assembly. In: 18th international conference on advanced robotics (ICAR); 2017. p. 61–7.
[14] Koren Y. General RMS characteristics. Comparison with dedicated and flexible systems. In: Dashchenko AI, editor. Reconfigurable manufacturing systems and transformable factories. Berlin, Heidelberg: Springer; 2006. p. 27–45.
[15] Wang H, Rong YK, Li H, Shaun P. Computer aided fixture design: recent research and trends. Comput-Aided Des 2010;42(12):1085–94.
[16] Shirinzadeh B. Issues in the design of the reconfigurable fixture modules for robotic assembly. J Manuf Syst 1993;12(1):1–14.
[17] Erdem I, Helgosson P, Kihlman H. Development of automated flexible tooling as enabler in wing box assembly. Proc CIRP 2016;44:233–8.
[18] Gödl M, Kovac I, Frank A, Haring K. New robot guided fixture concept for reconfigurable assembly systems. In: International conference on changeable, agile, reconfigurable and virtual production; 2005. p. 1–7.
[19] Jonsson M, Ossbahr G. Aspects of reconfigurable and flexible fixtures. Prod Eng 2010;4:333–9.
[20] Xiong L, Molfino R, Zoppi M. Fixture layout optimization for flexible aerospace parts based on self-reconfigurable swarm intelligent fixture system. Int J Adv Manuf Technol 2013;66(9–12):1305–13.
[21] Lu C, Zhao H-W. Fixture layout optimization for deformable sheet metal workpiece. Int J Adv Manuf Technol 2015;78(1–4):85–98.
[22] Camelio JA, Hu SJ, Ceglarek D. Impact of fixture design on sheet metal assembly variation. J Manuf Syst 2004;23(3):182–93.
[23] Li B, Melkote SN. Improved workpiece location accuracy through fixture layout optimization. Int J Mach Tools Manuf 1999;39(6):871–83.
[24] Krishnakumar K, Melkote SN. Machining fixture layout optimization using the genetic algorithm. Int J Mach Tools Manuf 2000;40(4):579–98.
[25] Prabhaharan G, Padmanaban KP, Krishnakumar R. Machining fixture layout optimization using FEM and evolutionary techniques. Int J Adv Manuf Technol 2007;32(11–12):1090–103.
[26] Xie W, Deng Z, Ding B, Kuang H. Fixture layout optimization in multi-station assembly processes using augmented ant colony algorithm. J Manuf Syst 2015;37:277–89.
[27] Tohidi H, AlGeddawy T. Planning of Modular Fixtures in a Robotic Assembly System. Proc CIRP 2016;41:252–7.
[28] Tadic B, Vukelic D, Miljanic D, Bogdanovic B, Macuzic I, Budak I, et al. Model testing of fixture-workpiece interface compliance in dynamic conditions. J Manuf Syst 2014;33(1):76–83.
[29] Kong Z, Ceglarek D. Fixture workspace synthesis for reconfigurable assembly using procrustes-based pairwise configuration optimization. J Manuf Syst 2006;25(1):25–38.
[30] Wan X-J, Li Q, Wang K. Dimensional synthesis of a robotized cell of support fixture. Robot Comput-Integr Manuf 2017;48:80–92.
[31] Cirillo A, Cirillo P, De Maria G, Marino A, Natale C, Pirozzi S. Optimal custom design of both symmetric and unsymmetrical hexapod robots for aeronautics applications. Robot Comput-Integr Manuf 2017;44:1–16.
[32] Caro S, Dumas C, Garnier S, Furet B. Workpiece placement optimization for machining operations with a KUKA KR270-2 robot. In: IEEE international conference on robotics and automation (ICRA); 2013. p. 2921–6.
[33] Tubaileh AS. Layout of robot cells based on kinematic constraints. Int J Comput Integr Manuf 2014;28:1–13.
[34] Hassan M, Liu D, Paul G, Huang S. An approach to base placement for effective collaboration of multiple autonomous industrial robots. In: IEEE international conference on robotics and automation (ICRA); 2015. p. 3286–91.
[35] Spensieri D, Carlson JS, Bohlin R, Kressin J, Shi J. Optimal robot placement for tasks execution. Proc CIRP 2016;44:395–400.
[36] Gadaleta M, Berselli G, Pellicciari M. Energy-optimal layout design of robotic work cells: potential assessment on an industrial case study. Robot Comput-Integr Manuf 2017;47:102–11.
[37] Michniewicz J, Reinhart G. Cyber-Physical-Robotics –Modelling of modular robot cells for automated planning and execution of assembly tasks. Mechatronics 2016;34:170–80.
[38] Zhang J, Fang X. Challenges and key technologies in robotic cell layout design and optimization. Proc Inst Mech Eng Part C J Mech Eng Sci 2017;231(15):2912–24.

[39] Doan NCN, Lin W. Optimal robot placement with consideration of redundancy problem for wrist-partitioned 6R articulated robots. Robot Comput-Integr Manuf 2017;48:233–42.
[40] Lim ZY, Ponnambalam S, Izui K. Multi-objective hybrid algorithms for layout optimization in multi-robot cellular manufacturing systems. Knowl-Based Syst 2017;120:87–98.
[41] Tsarouchi P, Michalos G, Makris S, Athanasatos T, Dimoulas K, Chryssolouris G. On a human–robot workplace design and task allocation sytem. Int J Comput Integr Manuf 2017;30(12):1272–9.
[42] Kovač I, Cardan joint, patent application EP2018060387W, European Patent Office (2018).
[43] Merlet J-P. Parallel robots. Dordrecht: Springer; 2006.
[44] Gilbert EG, Johnson DW, Keerthi SS. A fast procedure for computing the distance between complex objects in three-dimensional space. IEEE J Robot Autom 1988;4 (2):193–203.
[45] Eberly D. 3D game engine design: a practical approach to real-time computer graphics. Boca Raton, FL: CRC Press; 2006.
[46] Gill PE, Murray W, Wright MH. Numerical linear algebra and optimization, vol. 1. Redwood City, CA: Addison-Wesley; 1991.
[47] Spellucci P. A new technique for inconsistent QP problems in the SQP method. Math Methods Oper Res 1998;47(3):355–400.
[48] Byrd RH, Hribar ME, Nocedal J. An interior point algorithm for large-scale nonlinear programming. SIAM J Optim 1999;9(4):877–900.
[49] Abdel-Malek K, Yu W, Yang J, Nebel K. A mathematical method for ergonomic-based design: placement. Int J Ind Ergon 2004;34(5):375–94.
[50] Meike D, Pellicciari M, Berselli G. Energy efficient use of multirobot production lines in the automotive industry: detailed system modeling and optimization. IEEE Trans Autom Sci Eng 2014;11(3):798–809.
[51] Husty ML. An algorithm for solving the direct kinematics of general Stewart-Gough platforms. Mech Mach Theory 1996;31(4):365–80.
[52] Shoemake K. Euler angle conversion. In: Heckbert PS, editor. Graphics gems IV. San Diego, CA: Academic Press; 1994. p. 222–9.
[53] Murray RM, Li Z, Sastry SS. A mathematical introduction to robotic manipulation. CRC Press; 1994.